ELSEVIER

Thermochimica Acta 377 (2001) 141–150

thermochimica acta

www.elsevier.com/locate/tca

Temperature-modulated differential scanning calorimetric measurements on nascent ultra-high molecular mass polyethylene

G.W.H. Höhne*, L. Kurelec

Eindhoven Polymer Laboratories, The Dutch Polymer Institute, Eindhoven University of Technologie, P.O. Box 513, 5600 MB Eindhoven, The Netherlands

Received 18 December 2000; received in revised form 27 February 2001; accepted 1 March 2001

Abstract

Temperature-modulated differential scanning calorimetric (TMDSC) measurements on nascent ultra-high molecular mass polyethylene (UHMMPE) in scanning as well as quasi-isothermal mode are presented. From these measurements, a special irreversible relaxation process in the pre-melting region can be separated, which only occur on the first heating of the nascent material. The frequency dependence of this process yield a characteristic time constant of 6.5 s (or 24 mHz) which fits with the α_2-process known from mechanical measurements. Quasi-isothermal measurements show that there are two slow (exponential) relaxation processes with time constants of 2–5 and several hundred minutes, respectively. The latter is only found in the first run of nascent UHMMPE and seems to be connected with irreversible structural changes (crystal thickening and ordering). The low activation energy (ca. 50 kJ mol^{-1}) points to a chain diffusion process rather than melting and crystallization.

Keywords: Temperature-modulated DSC; Ultra-high molecular mass polyethylene; Relaxation process; Complex heat capacity

1. Introduction

Calorimetry offers the possibility to get information about processes taking place in materials if heat is exchanged with the surroundings. Conventional differential scanning calorimetry (DSC) measures the heat flow rate into a sample on heating it at a given rate:

$$\Phi(T,t) = C_p(T)\frac{\mathrm{d}T}{\mathrm{d}t} + \Phi^{\mathrm{ex}}(T,t) \tag{1.1}$$

The first term on right side characterizes the heat flow connected with the heat capacity C_p, of the sample (dT/dt: heating rate), this term is always greater than zero. The second term, the excess heat flow rate, contains all heat flow from processes possibly occurring in the sample (melting crystallization, chemical reactions, etc.). Such processes are usually combined with enthalpy changes which require the exchange of ''latent heat'' with the surroundings. If there are different processes occurring in parallel, the DSC measures the net heat flow rate of all processes.

The separation of the heat capacity part from the total signal is straight forward, as C_p does not change very much with temperature, this contribution can be approximated by a straight line (the baseline) which can easily be subtracted from the total signal. The situation is more complicated, if different processes contribute to Φ^{ex}, for example, if exothermic and endothermic processes (e.g. crystallization and melting)

* Corresponding author. Tel.: +49-7392-706710; fax: +49-7392-706712.
E-mail address: gwh.hoehne@t-online.de (G.W.H. Höhne).

0040-6031/01/$ – see front matter
PII: S0040-6031(01)00549-4

occur in the same moment. In such cases,the net excess heat flow rate may be about zero in a DSC, though such processes occur in the sample simultaneously they are not visible in the measured curve.

The method of temperature-modulated DSC (TMDSC) offers the possibility to separate time-dependent processes (with a non-zero complex excess heat capacity) from normal (static) heat capacity and latent heat signals which are time-independent or very fast compared to the time scale of modulation.

From polymers it is known, that pre-melting and re-crystallization takes place on heating well below the real melting region. These materials seem to be very interesting materials to be investigated with TMDSC. In particular, polyethylene (PE) is a material with very high chain mobility already well below the melting region. A special material, nascent ultra-high molecular mass polyethylene (UHMMPE), is recently in the center of interest. This material is synthesized in solution at rather low temperatures (well below the crystallization temperature) with Natta–Ziegler catalysts. The synthesis conditions cause nearly immediately crystallization of the chain running out of the active center of the catalyst. The outcome are conglomerates of poorly ordered crystals of very long chains with a rather low number of entanglements and a low number of inter-crystal molecules. This raw substance offers some very interesting possibilities to get a polyethylene material with high quality mechanical properties [1]. The chain mobility seems to be high in nascent UHMMPE this makes crystal growth and perfection on annealing possible well below the melting point. To get more insight into the nature of this process, we performed temperature-modulated differential scanning calorimetric (TMDSC) experiments with nascent UHMMPE. The aim of this paper is to show the power of this method for investigations of time-dependent processes resulting in a non-zero apparent heat capacity.

2. The TMDSC method

We used a standard Perkin-Elmer DSC-7 which we modified (using a precision function generator) to enable a sinusoidal temperature modulation:

$$T(t) = T_0 + \beta_0 t + T_A \sin(\omega t) \tag{2.1}$$

with a certain ''underlying'' heating rate β_0, a temperature amplitude T_A and the angular frequency $\omega = 2\pi f$ (f: frequency).

The measured (modulated) heat flow signal $\Phi(t)$ was first treated as usual [2]. By ''gliding integration'' over one period, we got the ''underlying'' part $\Phi_0(t)$ which is subtracted from the measured signal to get the periodic part:

$$\Phi_{per}(t) = \Phi(t) - \Phi_0(t) \tag{2.2}$$

The underlying part is identical to the signal one would get from conventional DSC with the same measuring conditions. The periodic part:

$$\Phi_{per}(t) = \phi_A(t)\cos(\omega t + \varphi) \tag{2.3}$$

was evaluated further, using the mathematical method deduced from lock-in amplification techniques [3], to get the amplitude Φ_A and the phase shift φ (relative to the temperature change) of that function.

From the amplitude Φ_A, we got the magnitude (modulus, absolute value):

$$|C_p| \equiv C_p = \frac{\Phi_A}{(T_A\omega)} \tag{2.4}$$

of the apparent (related to the modulation) complex heat capacity, which together with the phase φ reads:

$$C_p^*(t) = C_p\, e^{i\varphi} \tag{2.5}$$

Remark: complex quantities are marked with a^* within this paper, whereas the real valued magnitude (absolute value) is referred to without the upper star.

The phase of the complex heat capacity is disregarded in this paper, because the precise calibration of this quantity makes still problems. The C_p-magnitude of the apparent heat capacity has two components again:

$$C_p(T,t) = c_p(T)m + C_p^{ex}(T,t) \tag{2.6}$$

One part, the first term on the right side, is determined by the conventional (static) specific heat capacity $c_p(T)$ (>0) of the sample which always causes a heat flow in phase with the temperature change dT/dt. This static component is always present, it has normally only a very weak temperature dependence. The excess heat capacity, the second term on the right side, contains the heat flow from all processes which react significantly on the small temperature

changes of the modulation. In other words for these processes, the heat flow involved changes when the temperature (heating rate) changes, it follows the temperature change. Such processes are normally time-dependent as well. But there is a non-zero contribution only, if the time constant is not too slow compared to the time scale of the modulation (the period). If the time constant is within the same order of magnitude, the heat flow connected with the excess heat capacity is shifted in phase which causes a non-zero imaginary part of the (complex) heat capacity.

The apparent heat capacity determined from the modulated part of the signal is also called ''reversing heat capacity'' in literature, because it is determined from that part of the heat flow signal which is caused by the periodical changing (reversing) temperature. *Remark*: the term ''reversing'' must not be mixed up with ''reversible'' in the thermodynamic sense, in fact, the reversing heat capacity contains in its excess part often irreversible components.

It should be emphasized that the excess heat capacity from Eq. (2.6) does not contain all of $\Phi^{ex}(T, t)$ from Eq. (1.1), but only a certain fraction namely that part which changes with temperature modulation having the proper time constant. The fraction may change if we change the period (frequency) of the experiment. *Remark*: a time-dependent apparent heat capacity is equivalent to a frequency dependence in Fourier space. The contribution from processes with no or only very weak temperature dependence to $\Phi^{ex}(T, t)$ is found in the underlying signal (for instance from processes like crystallization or chemical reactions). Unfortunately, the separation of the contributions into temperature and time-dependent components is neither complete nor linear (additive) and depends, in addition, on the period (frequency) used in the experiment.

Generally, the deconvolution of the excess heat flow into the different time and temperature-dependent processes is a tricky and not so easy task. However, the method of TMDSC offers the possibility to separate processes with different temperature and time dependence from one another and determine characteristic quantities (like the time constant) from their frequency dependence. The evaluation of the TMDSC measurements done with nascent UHMMPE may serve as an example.

3. Experimental

Different types of nascent UHMMPEs have been investigated. In this paper, we confine ourselves to present the results from a special nascent UHMMPE (M_w ca. 4 Mio) from DSM (The Netherlands). The reactor powder has been investigated as received. Samples of 0.7–3.5 mg mass were weighted with a precision balance and encapsulated in standard (crimped) Al-pans of well known (and always the same) mass. Almost identical empty pans were used in the reference side and for the baseline run. Nitrogen was used as purge gas at a rate of 25 ml min^{-1}.

For TMDSC measurements, we used an underlying heating rate of 0.1 or 0.5 K min^{-1}, which was proved to be low enough to ensure no influence on the modulated part of the signal. Different frequencies in the range between 2 and 125 mHz were used to prove the frequency influence on the results. The temperature amplitude T_A was selected low enough to ensure linear response and in such a way, that the heating rate (the derivative of Eq. (2.1)) was always >0 and the same for the different frequencies (ωT_A = constant). This was done to exclude possible influences of a changed heating rate on the processes in the sample and the measurements. From the sample run results, the empty pan run results (taking the same measuring parameters and phase position) were subtracted before further evaluation, to reduce surroundings and apparatus influences.

Calculation of the apparent heat capacity (magnitude and phase) from the measured heat flow rate was done with a Windows™ program using the mathematical procedure described in [3]. The proper (frequency-dependent) calibration factor for the heat capacity magnitude, needed to correct for errors caused by heat transfer influences [4], was determined by comparing the calculated heat capacity in the liquid state with the respective value from literature [5].

4. Results

In Fig. 1, the magnitude and phase shift of the apparent heat capacity of nascent UHMMPE is plotted together with the c_p curve calculated from the underlying heat flow (which equals a conventional DSC measurement). Obviously, the magnitude curve differs

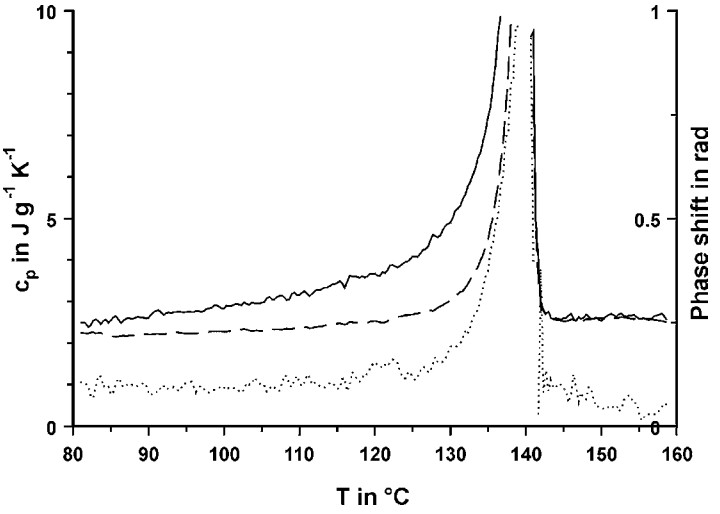

Fig. 1. TMDSC curves of nascent UHMMPE (mass: 1.6 mg, heating rate: 0.5 K min^{-1}, frequency: 12.5 mHz, T_A: 53 mK; solid line: c_p-magnitude, dotted line: phase shift, dashed line: underlying apparent c_p).

from the underlying curve in the pre-melting temperature region. There must be an excess heat capacity in that region which is only visible in the modulated (reversing) part of the heat flow signal, but not in the underlying curve.

To get more information about the process causing this excess heat capacity, we compared the magnitude curve from the first heating run with those of the respective cooling and second heating runs (Fig. 2). In the temperature region between 90 and 120°C, the first heating of the virgin material gives the largest excess heat capacity. This is distinctly smaller for the cooling run from the melt and the following second heating run (at least in the temperature region before melting starts). The smallest excess heat capacity is found for the c_p curve calculated from the

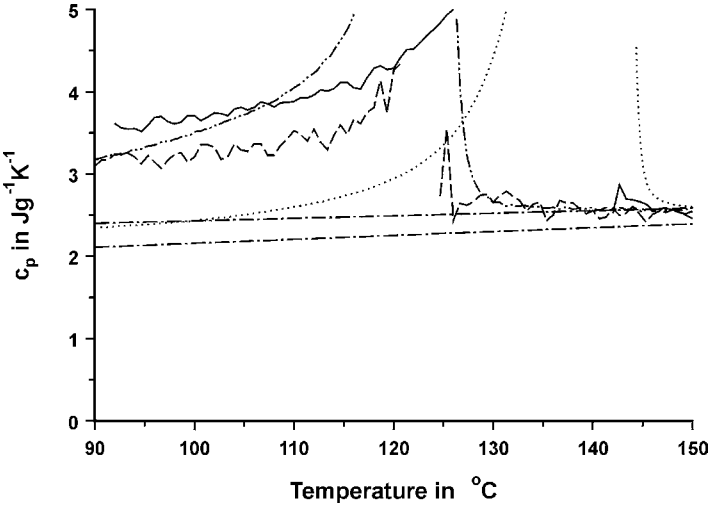

Fig. 2. TMDSC heat capacity curves of nascent UHMMPE on first heating (solid) subsequent cooling (dashed) and second heating (dash-dot-dotted) together with the conventional DSC curve at 10 K min^{-1} (dotted) and literature values of static c_p (crystal and amorphous phase, dash-dotted [5]) (mass: 0.7 mg, heating rate: 1.0 K min^{-1}, frequency: 12.5 mHz, T_A: 106 mK).

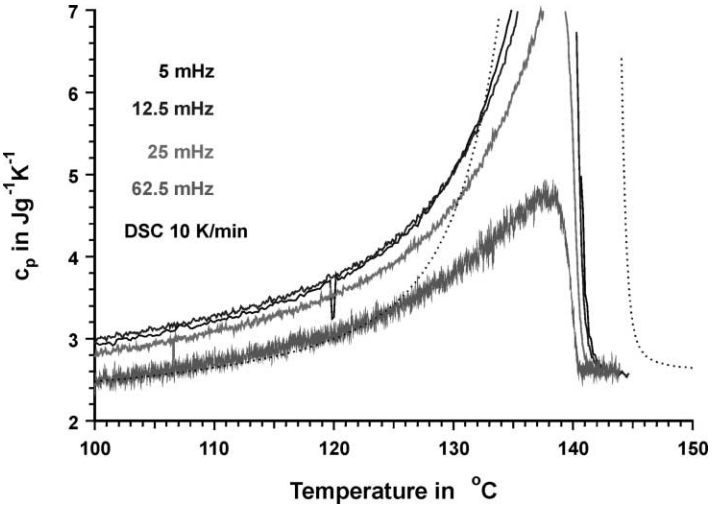

Fig. 3. TMDSC heat capacity curves of nascent UHMMPE on first heating at different frequencies together with the conventional DSC curve at 10 K min^{-1} (dotted) (mass: ca. 4 mg, heating rate: 0.1 K min^{-1}, $\omega T_A = 3.6$ mK rad s^{-1}).

conventional DSC run (which is like the underlying c_p curve). To get an impression of the static (thermodynamic) heat capacity of the sample, the literature values for the amorphous and crystalline phase of PE [5] are included in the figure. The real static heat capacity of the semi-crystalline sample is between these limiting curves and can be calculated with the known degree of crystallinity. In accordance with Eq. (2.6), the excess heat capacity is defined as the difference between the latter and the measured c_p curves.

From the results in Fig. 2 follows, that there must be two processes, at least, which contribute to the measured excess heat capacity. One of them exist only on heating the nascent UHMWPE the first time. It is characterized by the difference between the first heating and the cooling (or second heating) curves.

To get more information about the processes in question, we investigated the behavior at different frequencies. The results are shown in Fig. 3 with increasing frequency the excess heat capacity drops to the value of the underlying curve (Fig. 4). The processes are obviously time-dependent, they can not follow the temperature changes from the modulation anymore if the frequency is too large: the excess heat capacity drops to zero.

To get more details out of the measured frequency behavior, e.g. the time scale in question, we have to know the time-law of the process. The most basic formulation of a time dependence starts from a simple relaxation (retardation) process connected with an energy change which is described by

$$Q(t) = Q_0\, \mathrm{e}^{-(t/\tau)} \tag{4.1}$$

with τ the time constant and Q_0 the start value.

The heat flow involved (and exchanged) is the first derivative of the heat:

$$\Phi(t) = \frac{\mathrm{d}Q(t)}{\mathrm{d}t} = \frac{\mathrm{d}}{\mathrm{d}t} Q_0\, \mathrm{e}^{-(t/\tau)} = -\frac{Q_0}{\tau}\, \mathrm{e}^{-(t/\tau)} \tag{4.2}$$

To get the frequency dependence of such a process we have to Fourier transform this equation (see textbooks):

$$\Phi^*(\omega) \propto \frac{-1}{1 - \mathrm{i}\omega\tau} \tag{4.3}$$

The magnitude of the complex function $\Phi(\omega)$ scales like:

$$|\Phi^*(\omega)| = \Phi(\omega) \propto \frac{1}{\sqrt{1 + \omega^2\tau^2}} \tag{4.4}$$

The amplitude of the respective part of the modulated heat flow scales in the same manner. In TMDSC, the apparent heat capacity is calculated with Eq. (2.4). As the product ωT_A is kept constant during our measurements, C_p is proportional to Φ_A, i.e. it follows the same

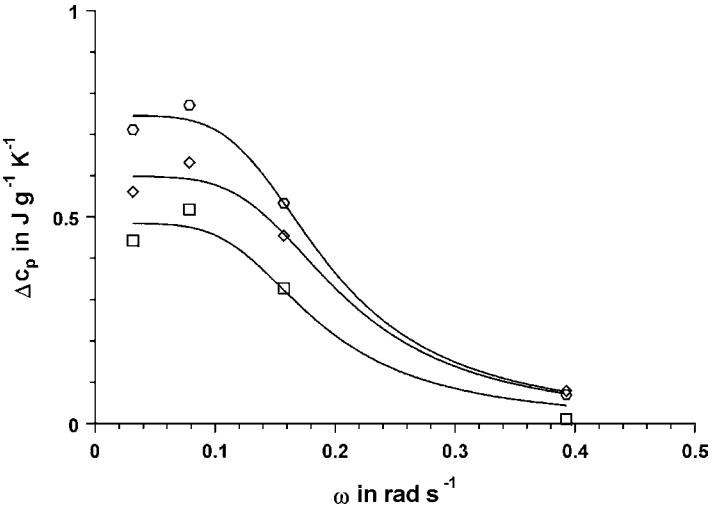

Fig. 4. Change of the difference of apparent heat capacities from modulated and underlying heat flow rate with frequency (squares: 100°C, diamonds: 110°C, hexagons: 120°C, solid lines: fit function similar to Eq. (4.4)).

type of law. Such a frequency dependence (see Fig. 4, solid lines) looks like the behavior, we found, consequently, the corresponding process may be a relaxation process and the excess heat capacity can therefore be formulated as

$$C_p^{\mathrm{ex}} = C_{p,0}^{\mathrm{ex}}\, \mathrm{e}^{-(t/\tau)} \tag{4.5}$$

with $C_{p,0}^{\mathrm{ex}}$ the start value at $t = 0$ and τ the time constant.

However, as stated in Section 2, we would not measure an excess heat capacity if the process is not somehow temperature-dependent. The simplest way to get the temperature in, is to take the time constant τ itself temperature-dependent. Again we have to make an assumption how this dependence may look like, to get more information. If the process is thermal activated (Arrhenius behavior) we can start from the following law:

$$\tau = \tau_0\, \mathrm{e}^{-(E_\mathrm{a}/RT)} \tag{4.6}$$

with E_a activation energy and R gas constant. To determine the proper time constant τ, as well as the activation energy E_a, we have to perform quasi-isothermal measurements at different temperatures in the region of interest. The results are shown in Fig. 5, obviously, the excess heat capacity changes with temperature and in time. With a proper mathematical fitting program, the curves can be further analyzed. For the 130°C measurement, we found that a sum of two exponential functions with different time constants is able to describe the measured curves within the limits of our measurement accuracy (which of course are somewhat noisy) (see Fig. 5). Taking this finding as true for the other temperatures as well, we got the data listed in Table 1. Because of the rather small (but nevertheless, significant) changes of the amplitude within the rather short measuring time these values are speculative and not very accurate (±10%), but it seems to be the simplest evaluation, for the highest temperature this is evident and the tendency is clear.

The first exponential (with the shorter time constant) may be connected with the heat transfer from the apparatus to the sample. On every sudden change from

Table 1
Evaluation of the curves from Fig. 5 as a sum of two exponential functions

Temperature T (°C)	Initial excess c_p (J g^{-1} K^{-1})		Time constants τ (min)	
90	0.6	1.1	5	760
100	0.4	1.1	1.5	610
110	0.4	1.0	2.5	510
120	0.4	1.1	3.5	360
130	0.1	1.1	4	165

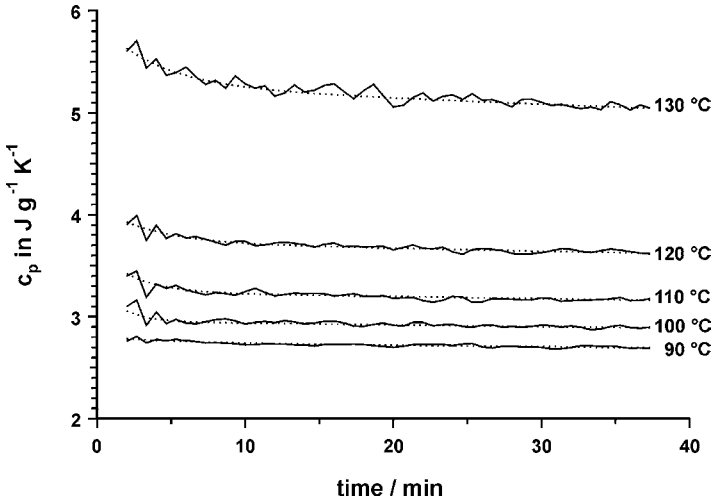

Fig. 5. C_p-magnitude curves from quasi-isothermal TMDSC measurements of nascent UHMMPE at different temperatures together with the fit (dotted) of two exponential curves with values of Table 1 (mass: ca. 3 mg, frequency: 12.5 mHz, T_A: 53 mK).

ambient to the isothermal measuring temperature, the DSC needs always some time to come to equilibrium conditions. This time constant depends on the measuring and initial conditions of the DSC (and the temperature step width from load to isothermal condition) rather than on the measuring temperature in question. These conditions were unfortunately, not kept identically for all experiments what may have caused the unsystematic scatter of this time constant. Our DSC needs some minutes after starting a run to come to steady-state conditions (even for conventional runs). This is the simplest interpretation of the first decrease of the measured magnitude and we prefer it rather than to assume a relaxation process of the sample. This is further supported by our finding that such an exponential is found for a sapphire sample as well, which surely do not contribute with a time-dependent heat capacity.

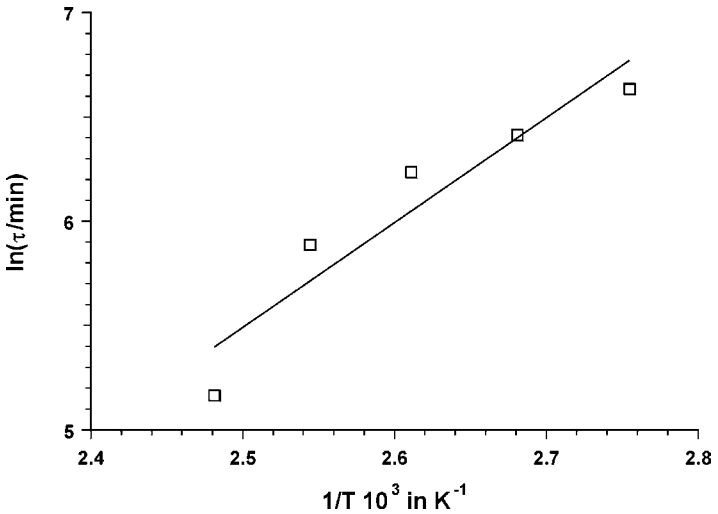

Fig. 6. Activation plot of the time constants determined from quasi-isothermal TMDSC measurements (Table 1).

The second time constant characterizes undoubtedly, a time-dependent process occurring in the sample itself (like in Eq. (4.5)). This time constant depends significantly on temperature. The related initial excess c_p is the total change of excess heat capacity (for infinite times) connected with the exponential decay of this process (Table 1). This quantity depends obviously not on the temperature chosen for the experiment, but on the nascent state of the sample, as it is connected with the first run only.

To prove the validity of the assumed law of Eq. (4.6) for this process, we have to plot $\log \tau_2$ against $1/T$ (see Fig. 6) which should result in a straight line with slope E_a/R. The result has this tendency, but only roughly. Even if we take the large error into account, there is a significant deviation from the Arrhenius behavior (Eq. (4.6)). However, from the (mean) slope of the linear approximation we find an ''activation energy'' of roughly 40 kJ mol^{-1} for the process which takes place on annealing the sample at the named temperatures.

From the frequency dependence of the excess heat capacity (see Fig. 4), on the other hand, we determined a third time constant of 6.5 ± 0.5 s taking a behavior like Eq. (4.4) into account. With $\omega_0 = 1/t = 0.15$ and $\omega_0 = 2\pi f$,we get the ''corner frequency'' (maximum of the imaginary part, where the amplitude drops to about 50% of the low frequency value) of that process$f_0 = 0.024$ Hz at 110°C.

5. Discussion

The objective of this paper is to show that there is a special time-dependent excess heat capacity in nascent UHMMPE (what is equivalent to a complex excess heat capacity in frequency domain) and the TMDSC method is a suitable method to get insight into this process. A detailed interpretation from the view point of polymer science would go beyond the scope of this article and will be published elsewhere [6]. Consequently, the discussion seems to be highly speculative in what follows, but we would, however, like to present it here for the interested reader.

With the TMDSC method used, there are different processes found in the pre-melting temperature region which contribute to the excess heat capacity of UHMMPE:

1. from the frequency dependence of the total TMDSC excess heat capacity (the difference between the absolute value of complex heat capacity and the underlying c_p value), we got a time constant of 6.5 s (24 mHz in frequency domain) at 110°C.
2. from isothermal TMDSC experiments we found, that there is a time-dependent process taking place which decreases the magnitude of a certain excess enthalpy (exponentially) in time scales of several hundred minutes. The corresponding (irreversible) excess $c_p = 1.1$ J g^{-1} K^{-1} seems to be independent on temperature. This process is thermal activated and the activation energy is roughly 40 kJ mol^{-1}.
3. even in cooling runs there is a complex heat capacity which is lower than that of the first heating run, but higher than the underlying heat capacity (from conventional DSC) of the first run.
4. the magnitudes of all complex heat capacities are significantly higher than the static heat capacity of the partial crystalline PE.

How can we get these findings together into one picture of what happens in UHMMPE in the pre-melting region?

The first finding, the corner frequency of 24 mHz at 110°C, fits exactly to the so-called α_2-process of PE (see Fig. 7) which describes the diffusion of dislocations with cooperative *c*-axis shearing (as well as chain diffusion) through the crystals [7]. From the slope in the activation diagram (Fig. 7), we get an activation energy of 50 kJ mol^{-1} for this process. This low-frequency process, normally found with dynamical mechanical methods, is always present in PE. Normally, it is not sensitive to TMDSC methods because there is no heat flow connected with it, as the enthalpy remains constant. However, obviously, we find this process in TMDSC, so there must be an heat flow connected with it. As the net heat flow is very low in the pre-melting temperature region (see underlying curve in Fig. 1), we have to draw the conclusion that there must be an endothermic as well as exothermic component present in the underlying heat flow, but the balance is almost zero during the process occurring. The same must be true for the modulated part of the total heat flow, even here there must be an endothermic as well as exothermic component present. If the

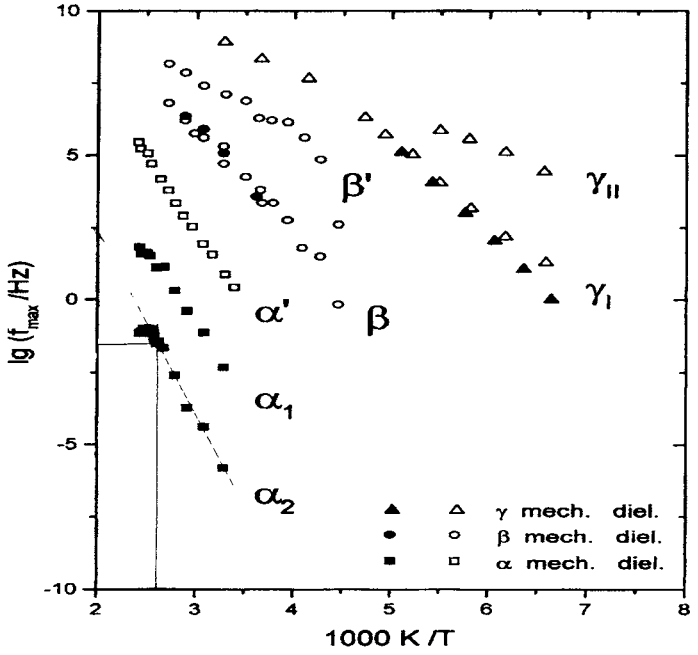

Fig. 7. Activation diagram of polyethylene [15]. The α-process takes place in the crystals, the β-process is the glass transition in amorphous and the γ-process is the local process. The ordinate lines mark the process found in TMDSC.

endothermic and exothermic heat flow follow the same time (and temperature) laws there will be no modulated net heat flow either. But if we start from, say, a law like Eq. (4.5) with different time constants for the endo- and exothermic heat flow there will be a non-zero excess heat capacity in the modulated signal as can be shown easily with proper model calculations.

If we take the activation energy of 50 kJ mol^{-1} into consideration, which equals the heat of fusion of 12 CH_2 groups using the literature value for PE with 4.1 kJ mol^{-1} repeating unit [5], we may explain the α_2-process of PE as a cooperative local "melting" and "crystallization" of ca. 12 CH_2. If we assume different time constants for the appearing and disappearing of this local disordering inside the crystals of PE, this would make the α_2-process visible in the TMDSC.

What is the slow irreversible process (2) during isothermal annealing then? The activation energy of 40 kJ mol^{-1} is (within the limits of our experimental accuracy) roughly the same as that of the α_2-process. We believe that chain diffusion through the crystal takes place in connection with the dislocation diffusion already well below the melting region. This leads to an ordering of the rather chaotic crystals of nascent UHMMPE (produced in the reactor at rather low temperatures), but without measurable change of the degree of crystallinity. Otherwise there should be a non-zero net heat flow in the underlying curve, which could not be found experimentally (see Figs. 1 and 2). Recent X-ray measurements [6], which showed a significant lamella thickening taking place during annealing at 120°C, support our assumption.

The activation energy of the process equals the "melting" of 9–12 CH_2 groups, this is far to small a number to speak about local melting and re-crystallization of a total lamella which contain at least 100 CH_2 groups in chain direction.

Reversible melting, which has been reported by other authors [8–12,16,17], leading to an excess heat capacity too (this is clearly visible in the modulated cooling run (Fig. 2)), may be present even at heating. It could be the remaining part of the excess heat capacity if we subtract the value of 1.1 J g^{-1} K^{-1} (Table 1) from the total excess heat capacity on heating.

Such a reversible melting seems, however, not to be the right explanation for the considered process which

takes place only during the first heating of the nascent material. Whereas reversible melting is reported to be always present with polyethylene [12,16,17] and even other polymers [13,14]. In the latter, the authors report about similar relaxation processes which could be describes with a Kohlrausch–Williams–Watts equation. We believe that our process is, however, a different one which exist in addition to their processes which may be present in UHMMPE as well, but has not been investigated yet. Recently, Androsch and Wunderlich reported about their results from PE-octane co-polymers [16,17] and listed six different processes contributing to the measured excess heat capacity. One of them, the crystal perfection, seems to be the most convincing explanation of the irreversible process, we found in UHMMPE. Chain diffusion, linked with the dislocation diffusion of the α_2-process, transforms the rather distorted crystal aggregates to nearly ideal crystallites. Such a process should take place at rather large time scales because of the large masses which must be transported and the constraints acting on the polymer chain. Ordering by single chain diffusion should leave the total degree of crystallinity almost unchanged and even the total enthalpy, that is the reason why the underlying curve does not show an excess heat flow rate.

The α_2-process itself, the movement of dislocations (which helps to transport the chain) is of course much faster (seconds) because it acts locally with a much smaller mass transport involved as is the case with the chain diffusion.

6. Conclusions

Temperature-modulated differential scanning calorimetry is a suitable method to study pre-melting processes in polymers. For nascent UHMMPE, it is possible to separate different processes only visible in the modulated heat flow signal as an excess time-dependent (and thus, complex) heat capacity whereas the net heat flow, as measured in conventional DSC, remains almost zero in this temperature region. There is only a small change of the degree of crystallinity detectable, much smaller than the time-integral over the excess heat capacity necessitates. Consequently, there must be a (time and temperature-dependent) process with a zero net heat flow, but different time constants of the heat consuming and heat providing steps of that process. One such process, which, obviously irreversibly, occurs during the first heating of nascent UHMMPE already well below the melting region, is a crystal ordering (with lamella thickening) by chain diffusion through the crystal via the α_2-process. The time constant is (depending on temperature) around 500 min the activation energy is ca. 40 kJ mol^{-1} a value which equals the fusion heat of about 9 CH_2 units. The excess heat capacity connected to this irreversible process is 1.1 J g^{-1} K^{-1} (independent on temperature) a value which is lower than the total excess heat capacity on heating. The remaining part of the excess heat capacity, which even exist in modulated cooling runs, may be connected to processes like reversible melting (or melting–crystallization) and reordering of small crystals.

References

[1] S. Rastogi, L. Kurelec, P.J. Lemstra, Macromolecules 31 (1998) 5022.
[2] B. Wunderlich, Y. Jin, A. Boller, Thermochim. Acta 238 (1994) 277–293.
[3] G.W.H. Höhne, Thermochim. Acta 304/305 (1997) 209–218.
[4] G.W.H. Höhne, Thermochim. Acta 330 (1999) 93–99.
[5] B. Wunderlich, et al., Athas databank (http://web.utk.edu/~athas).
[6] L. Kurelec, et al., Macromolecules, 2001, in preparation.
[7] Deformationsmechanik von Polyäthylen bis zur Fliessgrenze, in: Proceedings of the Deutscher Verband für Materialprüfung e.V. Aachen., 1975, p. 148.
[8] I. Okazaki, B. Wunderlich, Macromolecules 30 (1997) 1758–1764.
[9] A. Toda, C. Tomita, M. Hikosaka, Y. Saruyama, Polymer 39 (21) (1997) 5093–5104.
[10] Y. Saruyama, J. Therm. Anal. Cal. 59 (2000) 271–278.
[11] W. Hu, T. Albrecht, G. Strobl, Macromolecules 32 (1999) 7548–7554.
[12] Y. Saruyama, Thermochim. Acta 330 (1999) 101–107.
[13] A. Toda, T. Arita, M. Hikosaka, J. Mater. Sci. 35 (2000) 5085–5090.
[14] C. Schick, M. Merzlyakov, B. Wunderlich, Polym. Bull. 40 (1998) 297.
[15] P.U. Mayr, Ph.D. thesis, University of Ulm, 1998.
[16] R. Androsch, B. Wunderlich, Macromolecules 32 (1999) 7238–7247.
[17] R. Androsch, B. Wunderlich, Macromolecules 33 (2000) 9076–9089.